Ultrasonic trapping in capillaries for trace-amount biomedical analysis

M. Wiklund[a)]
Biomedical and X-ray Physics, Royal Institute of Technology, S-100 44 Stockholm, Sweden

S. Nilsson
Technical Analytical Chemistry, Lund Institute of Technology, P.O. Box 124, S-221 00, Lund, Sweden

H. M. Hertz
Biomedical and X-ray Physics, Royal Institute of Technology, S-100 44 Stockholm, Sweden

(Received 30 August 2000; accepted for publication 5 April 2001)

A longitudinal hemispherical standing-wave ultrasonic trap for size-selective separation of microspheres in small-diameter capillaries is described. The trap utilizes the competition between acoustic radiation forces and viscous drag forces on spheres suspended in a liquid inside 20–75-μm-diam fused silica capillaries. Experiments performed on 3.0- and 4.7-μm-diam latex spheres demonstrate the principles of trapping and verify the theoretically calculated size-dependent forces on the spheres. The spheres are detected by the use of laser-induced fluorescence. The goal is to use the trap for separation and ultrahigh-sensitivity detection of trace amounts of proteins and other macromolecules containing two antigenic sites, by binding the target molecule with high specificity to antibody-coated latex spheres. © *2001 American Institute of Physics.*
[DOI: 10.1063/1.1376412]

I. INTRODUCTION

Nonintrusive manipulation by standing-wave acoustics has been widely used for levitation and trapping of macroscopic objects.[1] The standing-wave field creates an acoustic radiation force on the object that depends on its size and acoustic parameters.[2] In the present article we demonstrate size-selective separation and retention of latex spheres inside a small-diameter flow-through capillary by use of an ultrasonic radiation trap. The work aims at rapid in-flow detection and separation of specific molecules via antibody-coated latex spheres.

Acoustic radiation forces have been used for nonintrusive manipulation of macroscopic as well as microscopic objects. Basically, objects with higher acoustic impedance than the surrounding medium are trapped in the velocity antinodes of the standing-wave acoustic field. The theory of acoustic levitation and trapping is well understood.[2,3] In aqueous solutions the method has been applied for studies of mechanical properties of mm- to μm-sized liquid droplets and biological cells.[4,5] These experiments typically operate at low frequencies (kHz up to a few 100 kHz) using a closed cylinder levitation vial. Similar systems have been used for cell concentration,[6] cell filtering,[7] and for enhanced rate and sensitivity of latex agglutination tests by increasing particle collision rates.[8] Here few-mm-diam tubes or chambers are combined with a transverse acoustic field (propagation perpendicular to the length of the tube), resulting in a higher cell concentration in several velocity antinodes parallel with the tube. In-flow separation and fractionation of suspended particles are performed on the basis of size and/or acoustic properties with a liquid flow in combination with flow splitters.[9,10] Electric fields have been employed in a similar arrangement to transversely separate charged particles by exploiting the competition between acoustic radiation forces and electrostatic forces.[11] At higher ultrasonic frequencies ($>$10 MHz) acoustic traps based on a standing-wave confocal ultrasonic cavity have demonstrated that longitudinal forces of similar magnitude or higher than those of optical traps can be achieved.[12] Finally, it should be noted that low-frequency airborne acoustic traps have been used for improved biomedical analysis.[13]

In biomedical analysis, great effort is made to develop detection techniques of trace amounts of specific proteins and other biomolecules. Very small sample volumes (pl-nl) may be analyzed with narrow-bore sub-100 μm capillaries in combination with electrophoresis, capillary electrophoresis (CE), or capillary electrochromatography (CEC).[14] CE/CEC separates analytes according to charge, size, and chemical characteristic with high selectivity and high throughput. Typically, the limit of detection using fluorescent analytes is femtomols, which may be improved by several orders of magnitude in special cases.[15,16] The use of antibody-coated microspheres in CE/CEC may improve the selectivity and the detection limit of specific macromolecules.[17]

In the present article we introduce the combination of flow-through small-diameter capillaries and a high-frequency longitudinal ultrasonic trap, which allows microspheres to be separated according to size with high selectivity inside the capillary. This capillary ultrasonic trap utilizes the competition between acoustic radiation forces and viscous drag forces. Inside the capillary, these forces act in opposite directions on the spheres, resulting in size-selective trapping and in-flow separation. In the present article the separation efficiency of the system is theoretically analyzed. Furthermore, in a first proof-of-principle experiment the capillary ultrasonic trap is applied on differently sized fluorescent la-

a)Electronic mail: Martin.Wiklund@biox.kth.se

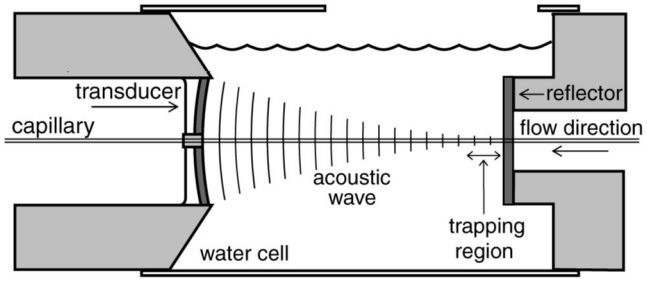

FIG. 1. Experimental arrangement for the capillary ultrasonic trap.

tex spheres suspended in water inside 20–75 μm quartz capillaries. The experiment demonstrates the size-selective trapping and verifies the applicability of the theory inside the capillary.

Longitudinal acoustic trapping has previously been combined with liquid flow in large-diameter tubes for fluid–particle separation and selection in, e.g., slurries.[18] The use of small-diameter capillaries allows smaller sample volumes and higher sensitivity, which is of importance for biomedical applications. The long-term goal of the present article is to improve the limit of detection of specific proteins or other sample molecules compared to current CE/CEC technology. Here two different monoclonal antibodies against two different antigenic sites on the analyte molecule will be covalently bound to different latex spheres. When the sample molecules are mixed with the two different latex spheres, a sandwich assay (latex-sample-latex complex) is formed with high specificity.[19] The size difference between the sandwich assay and single latex spheres may then be employed for separation and enrichment with the capillary longitudinal ultrasonic-trap system, allowing detection of minute concentrations of the target molecule. Compared to laser-optical trapping for similar purposes,[20] a longitudinal ultrasonic trap has the potential to provide a much more compact arrangement, and to produce a more uniform trapping field in smaller-diameter capillaries, which is important for high selectivity and sensitivity.

II. THEORETICAL BACKGROUND

In this section we theoretically analyze the forces acting on latex spheres in the capillary with an ultrasonic trap. The experimental arrangement is shown in Fig. 1 and will be described in more detail in Sec. III. For the theoretical background of this section it suffices to mention that a standing-wave ultrasonic trap is formed inside a capillary which contains a flow of a latex/water mixture. The two major competing forces on a latex sphere are due to the acoustic radiation force (F_{acoust}) and the viscous drag force (F_{visc}). Since the trap-generating ultrasonic beam is parallel with the capillary (and thus the flow direction), we will only consider forces parallel with the capillary (z axis). A more complete description would also include minor forces due to Brownian motion and gravity,[18] and the scattered acoustic field.[2] However, these forces are typically a few orders of magnitude smaller than F_{acoust} and F_{visc} (cf. Sec. V).

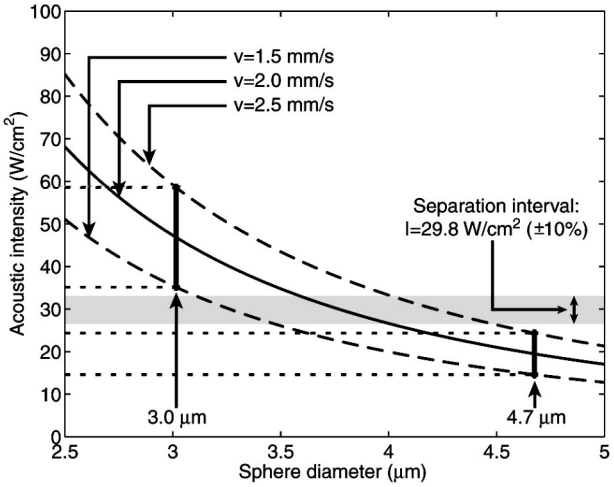

FIG. 2. Theoretical calculation of the acoustic intensity needed to trap latex spheres of diameters 3.0 and 4.7 μm traveling in water with velocities $v = 2.0$ mm/s $\pm 25\%$. Within the interval $I = 7.6$ W/cm$^2 \pm 10\%$, all 4.7-μm-diam spheres will be trapped, but none of the 3.0-μm-diam spheres.

The standing-wave acoustic forces on a sphere have been derived by several authors. Below we will quantitatively describe these forces following Refs. 2, 3, and 12. For a qualitative understanding it is useful to think of the acoustic radiation force as resulting from the gradient in an acoustic Bernoulli pressure. Thus, the sphere is trapped in the velocity antinodes of the standing-wave field. For a sphere considerably smaller than the acoustic wavelength, the force along the axial z axis is

$$F_{\text{acoust}} = \frac{VP_a^2}{4\rho_0 c_0^2}\left(\frac{1}{\delta\sigma^2} - \frac{5\delta - 2}{2\delta + 1}\right) k_z \sin(2k_z z), \tag{1}$$

where V is the particle volume, P_a is the peak acoustic pressure amplitude, and c_0 is the speed of sound in the liquid, $\delta = \rho/\rho_0$ where ρ and ρ_0 are the density of the sphere and the liquid, respectively, and $\sigma = c/c_0$ where c is the speed of sound in the particle. The term k_z is the wave number $2\pi/\lambda$, where λ is the acoustic wavelength. Thus, the axial acoustic force F_{acoust} is proportional to the z-axis gradient of the intensity I_a of the standing-wave acoustic beam via $I_a = P_a^2/2\rho_0 c_0$. In the present experiments the diameter of the acoustic beam is much larger than the narrow bore of the capillary. Thus, the radial acoustic intensity gradient perpendicular to the flow direction is small, resulting in that only axial forces need to be considered.

The acoustic force on a sphere acts in the opposite direction to the viscous drag force, which may be written

$$F_{\text{visc}} = 6\pi\eta v r, \tag{2}$$

where η is the viscosity, v the flow velocity, and r the particle radius. Thus, the acoustic force of Eq. (1) is proportional to r^3 (volume) while the viscous force is proportional to r. This is the basis for the separation properties of the device described in the present article. By properly adjusting the acoustic intensity, large-diameter spheres may be trapped in the capillary by a dominating acoustic force while for small-diameter spheres the viscous forces still may dominate, resulting in that they flow through the trap. Figure 2

shows a theoretical calculation based on Eqs. (1) and (2) of the necessary acoustic intensity for trapping spheres in a flow with velocity 2.0 ± 0.5 m/s, i.e., $\pm 25\%$. In the proof-of-principle experiments described below, a large majority or the latex spheres are observed in this velocity range. We especially indicate the difference in acoustic intensities necessary for trapping the sphere diameters 3.0 and 4.7 μm used in the present proof-of-principle experiments. Clearly, there is a significant interval in acoustic intensity in which size-selective trapping can be performed, despite the large velocity range. This is experimentally demonstrated in Sec. IV. The extension of the method to separate latex-protein-latex complexes is discussed in Sec. V.

III. EXPERIMENTAL ARRANGEMENT

The experimental arrangement of the capillary ultrasonic trap for size-selective separation is illustrated in Fig. 1. Basically it consists of a focusing transducer that creates a standing-wave pattern inside a quartz capillary by reflection in a plane acoustic reflector. The system is submerged in water to minimize acoustic reflection losses.

The transducer consists of a 8.5 MHz rf-amplifier-driven 20-mm-diam lead–zirconate–titanate focusing bowl (Pz27, Ferroperm, Denmark) with a radius of curvature of 50 mm, resulting in a ~400-μm-diam focused spot (cf. below). The acoustic trap is generated by a high-impedance molybdenum reflector (thickness 2 mm) placed in the focal plane, resulting in a hemispherical acoustic standing-wave arrangement. Molybdenum was chosen due to its high acoustic impedance, giving a reflectivity (water to molybdenum) of 91%.[21] The envelope of the water-filled chamber was a soft cylinder-shaped rubber cloth, allowing translation and rotation of the transducer and the reflector for alignment.

We used four different fused silica capillaries in the experiments (Polymicro Technologies, Arizona), with inner/outer diameters 75/126, 50/126, 40/81, and 20/66 μm. The capillary extended along the central axis of the acoustic field, through center holes in the transducer and the reflector. The arrangement results in a narrow, standing-wave, high-intensity acoustic field along the capillary in the region near the reflector. The reflector center hole was designed to fit each capillary dimension, just large enough to let the capillary through without damage. The matching of the dimensions of the capillary and the reflector hole is important to maximize the reflected intensity of the ~400 μm acoustic beam in the molybdenum plate around the capillary.

A high size selectivity requires a high uniformity of the standing-wave acoustic field. From scanning needle hydrophone measurements with a 75-μm-diam probe (Precision Acoustics Ltd., UK), the acoustic intensity profile in focus was determined to be close to Gaussian with a full width at half maximum of ~400 μm. Assuming a perfect Gaussian profile, the acoustic intensity varies approx. $\pm 0.1\%$ (20/66-μm-diam capillary) and approx. $\pm 1.2\%$ (75/126-μm-diam capillary) over the capillary inner cross section area. The thin walls of the quartz capillary (thickness approximately 0.1 times the acoustic wavelength in quartz) presumably results in evanescent-wave coupling of the acoustic waves into the capillary. Thus, a minimum of interference from the quartz walls is expected.

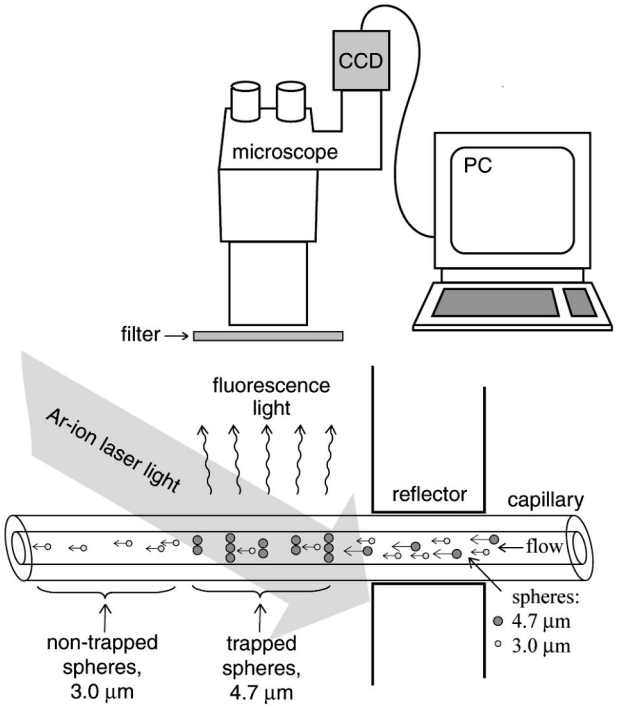

FIG. 3. Schematic illustration of the LIF detection system. The sample of mixed 4.7- and 3.0-μm-diam spheres enters the trap from the right-hand side. The 4.7-μm-diam spheres are trapped and detected in the LIF window, while the 3.0-μm-diam spheres elude from the trap.

The acoustic trap is aligned with precision stages by studying the trapping of powder near the reflector hole with the capillary removed, resulting in powder disks trapped in the velocity antinodes, longitudinally separated by ~90 μm ($\lambda/2$). When the alignment is optimized, the distance from the reflector hole to the first stably trapped disk is approximately 400 μm ($2-3\lambda$). The absence of trapped powder closer to the reflector is due to the negligible reflectivity of the water-filled hole. Further away, diffraction of the reflected wave allows a standing-wave pattern to be formed with the incident beam. Finally, the powder is removed and the capillary is mounted through the hole and, thus, in the trap.

As outlined in Secs. I and II, the goal of the experiments is to demonstrate the size-selective trapping of latex spheres in the capillary ultrasonic trap. For this purpose a laser-induced fluorescence (LIF) system was combined with the acoustic trap arrangement, as shown in Fig. 3. The requirement of the system is the ability to detect a single moving sphere throughout the depth of the capillary inner diameter, i.e., 20–75 μm.[22] We used fluorescent polystyrene carboxy-functionalized latex spheres (Polyscience Inc., PA) with diameters 4.7 and 3.0 μm (4.675 ± 0.208 and 3.015 ± 0.138 μm). The fluorescein-5-isothiocyanate 4.7 μm sphere had excitation maximum at $\lambda = 458$ nm and emission maximum at $\lambda = 530$ nm and the rhodamine 3.0 μm sphere, at $\lambda = 530$ and 570 nm, respectively. The excitation source was an Ar-ion laser (Coherent Innova 70-4) operated in multi-line mode with a maximum output power of 4 W. Via

narrow bandpass interference filters the $\lambda = 458$ nm or $\lambda = 514.5$ nm lines could be selected. The laser light was focused on the capillary with an angle of incidence $\sim 70°$, giving a cross section area projected on the capillary of approximately 0.3×1 mm. The fluorescence light from the spheres was separated from the laser light by a colored glass filter (OG550) and detected by a black-and-white charged coupled device (CCD) camera mounted on a $63\times$ microscope.

The interference filters were mounted on a wheel in front of the laser, allowing rapid change of excitation wavelength. With $\lambda = 458$ nm the 4.7 μm spheres produce strong fluorescence with very good signal-to-noise (S/N) ratio. The 3.0 μm spheres could not be excited by this laser line. The $\lambda = 514.5$ nm excitation light was moderately suitable for both spheres, resulting in a detectable fluorescence signal of equal strength for the two sphere sizes with a S/N$\approx$4. Naturally, improved spectral separation would have been advantageous since this would allow us to only detect the 3.0 μm spheres. Thus, by comparing pictures taken by the CCD using the two different excitation wavelengths, the sphere sizes could, in principle, be determined. Using the 458 nm line, only the big spheres are visible, but with the 514.5 nm line, both big and small spheres are visible.

The original latex suspensions, typically 2.5% latex by weight, were diluted in 25 mM sodium borate ($Na_2B_4O_7$), pH 9.2, to simulate typical CE conditions. We prepared samples with final concentrations of $5\times10^3-5\times10^4$ spheres/μl, corresponding to a mean distance between spheres of 30–60 μm. These samples are injected into the capillary. In order to generate a constant laminar flow inside the capillary, we used a motor-driven microliter syringe. During the experiments, the mean flow velocity inside the capillary, typically 0.5–3 mm/s, could be held constant, but, due to the parabolic velocity profile, the sphere velocity distribution spans from the maximum value on the capillary axis to almost zero near the inner wall. Still, the great majority of the observed sphere velocities were in the range $\pm$25%, as mentioned in Sec. II. The latex-suspension sample enters the trap from the reflector side, giving rise to an immediate, strong radiation force on the spheres. The reason to drive the flow from this direction is to avoid a gradually increasing acoustic force resulting in a risk of having spheres trapped before the fluorescence detection window.

IV. EXPERIMENTS

In order to investigate the function of the trap and the LIF detection system, experiments were performed with uniformly sized spheres. Figure 4 shows a typical view from the microscope with 4.7 μm spheres in a 75/126 μm capillary using the $\lambda = 458$ nm laser line. Initially, when the acoustic field is turned off, each sphere is clearly resolved, moving with the pressure-induced flow [Fig. 4(a)]. When a voltage is applied over the transducer, the acoustic force amplitude increases and when it reaches equilibrium with the viscous drag force, the spheres are trapped in positions of maximum acoustic intensity gradient. Due to the dominating gradient in the propagation direction of the acoustic field, the trapped spheres line up close together in a plane perpendicular to the capillary axis, and they are not individually resolvable [Fig. 4(b)]. When the transducer is turned off the trapped spheres move apart and they can be individually detected.

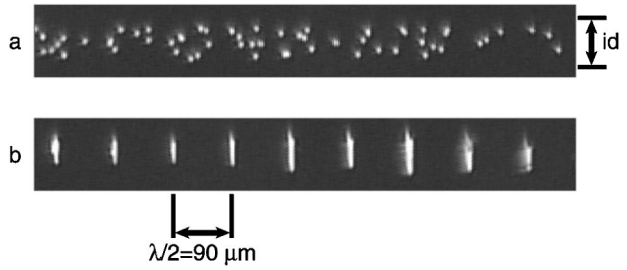

FIG. 4. Fluorescence images of 4.7-μm-diam latex spheres inside the $id = 75$ μm capillary without the acoustic trap (a) and with the acoustic trap (b) activated.

It is of interest to estimate the magnitude of the acoustic forces on the latex spheres that can be generated inside the capillary. This experiment was performed by recording consecutive CCD images of a flow of 3.0 μm spheres while increasing the transducer voltage until all spheres were trapped. From the CCD images the velocity, and, thus, the viscous-drag force F_{visc} [Eq. (2)], can be determined. At the transducer trapping voltage this force is exactly equal to the acoustic force F_{acoust} [Eq. (1)]. Thus, the acoustic intensity I_a inside the capillary may be calculated by combining Eqs. (1) and (2). With $I_a = P_a^2/2\rho_0 c_0$, this results in

$$I_a = k\frac{v}{r^2}, \tag{3}$$

where k is a constant. Equation (3) indicates the important experimental parameters, i.e., the sphere velocity (v), and the sphere radius (r). With a maximum velocity of 4 mm/s when trapping 3.0 μm spheres, Eq. (3) gives a maximum intensity $I_a = 90\ \text{W/cm}^2$ inside the capillary. This corresponds to an acoustic radiation force of 110 pN acting on the 3.0 μm spheres and 420 pN acting on the 4.7 μm spheres. Thus, it is clear that the acoustic forces are sufficiently large to allow trapping over a wide range of sphere sizes and flow velocities. To estimate the coupling efficiency of the focused acoustic wave into the capillary, the acoustic pressure amplitude in focus was measured by a 0.5 mm needle hydrophone (Precision Acoustic Ltd., UK) with the capillary removed. From this the standing-wave intensity without the capillary may be calculated. Naturally, there is no reflector and, thus, no standing wave in this case. Comparing this intensity outside the capillary with the measured value inside, results in a coupling efficiency on the order of 5%–10%.

The experiments demonstrating the size-selective separation efficiency were performed with samples of mixed sphere sizes, equal proportions of 3.0 and 4.7 μm spheres. Different capillaries were used with inner diameters ranging from 20 to 75 μm. Each experiment was documented by approximately 500 CCD pictures taken with a frequency of 8 Hz, i.e., 60 s each run. The mean velocity was held constant (0.5–3 mm/s) and the acoustic intensity was gradually increased until all 4.7 μm spheres were trapped. By rapidly changing the laser wavelength between 458 and 514.5 nm,

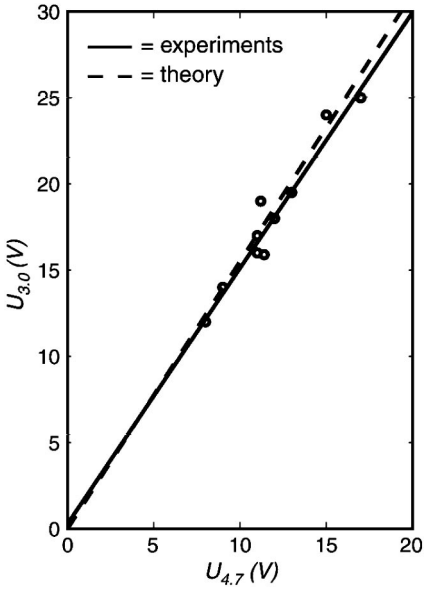

FIG. 5. Verification of theory. Each data point $(U_{4.7}, U_{3.0})$ represents the transducer voltages needed to trap 100% of 4.7- and 3.0-μm-diam spheres, respectively. The solid line is a linear least-square fit to the data points with slope 1.50. The slope of the dashed line is the ratio of the spheres diameters (1.55).

the size of each sphere could be determined. The results from all experiments indicate that the large majority of the 3.0 μm spheres were passing through the trap, when the acoustic intensity level was set just above the trapping level for all the 4.7 μm spheres. Still, a few percent of the low-velocity 3.0 μm spheres were trapped due to a decrease in the velocity-dependent viscous drag force near the capillary inner wall. From detailed video analyses, the maximum observed sphere velocity variation was $\pm 70\%$. Thus, with the parabolic flow profile of this experiment, a 100% trapping selectivity is not possible.

In order to compare the experimental results with theory, the applied transducer voltage was measured when trapping 4.7 and 3.0 μm spheres, respectively. The measurement procedure was similar to the one described above. First, we measured the transducer voltage when 100% of the 4.7 μm spheres were trapped $(U_{4.7})$ using the $\lambda = 458$ nm line, at constant mean velocity. Then we measured the voltage when all spheres (both 4.7 and 3.0 μm) were trapped $(U_{3.0})$ using the $\lambda = 514.5$ nm line, at the same velocity. Since $I_a \propto r^{-2}$ [Eq. (3)], $I_a \propto P_a^2$, and $P_a \propto U$, the theoretical relationship between the transducer voltages and the sphere sizes is

$$\frac{U_{3.0}}{U_{4.7}} = \frac{4.68\,\mu\text{m}}{3.02\,\mu\text{m}} = 1.55. \tag{4}$$

In Fig. 5, the transducer voltages $U_{4.7}$ and $U_{3.0}$ are plotted from different experiments, using different capillary sizes and flow velocities. The slope of the dashed line is the sphere radius ratio, 1.55. Fitting a straight line to the measured voltage data (least-square) gives a slope of 1.50. Given the uncertainty in latex sphere diameters (approx. $\pm 4.5\%$), the measured voltage ratio and the calculated sphere radius ratio are in good agreement, which confirms that the theoretical size dependence of the forces acting on the spheres also works inside the capillary.

V. DISCUSSION

We have demonstrated the principles of the capillary ultrasonic trap for size-selective separations. The results from the measurements indicate that it is possible to separate 4.7-μm-diam spheres from 3.0-μm-diam spheres, even with a nonuniform velocity distribution. We will now briefly consider the separation efficiency of particles with more similar diameters and especially the case of separating very few large particles among many small. This corresponds to the case of detecting trace amounts of two-particle latex-sample-latex complexes (doublets) from single latex spheres (singlets) as discussed in Sec. I. Here the acoustic force is a factor 2 larger for the doublet than for the singlet due the volume dependence of Eq. (1). The viscous drag force [Eq. (2)] for the doublet is determined by an effective radius of the complex. This varies between 1.3 and 1.4 times the radius of a singlet, depending on the orientation of the doublet in the flow.[23] At present we have no evidence for any specific orientation of the doublets. Performing a similar calculation as in Sec. II for this case assuming the same allowed acoustic intensity interval as in Fig. 2 ($\pm 10\%$), and an effective doublet radius of 1.4 times singlet radius (worst case), the maximum allowable sphere velocity interval will then be approx. $\pm 7\%$. Thus, in addition to a uniform acoustic field, the velocity distribution of the particles must be carefully controlled. A very uniform velocity distribution may be obtained by applying an electric field along the capillary resulting in an electro-osmotic flow, well known in CE. This produces a significant interval in which size-selective trapping is possible. With such uniform acoustic and flow fields the capillary ultrasonic trap has the potential to improve sensitivity in CE by allowing long sample enrichment and detection times at spatially specified positions in the capillary. Naturally, improving the uniformity of the acoustic field will relax the requirements on the velocity uniformity.

There is an upper limit of the trapping force in order not to also trap the singlets. This results in a certain possibility that the trapped doublets escape via Brownian motion. The escape may be modeled assuming that an isolated doublet moves stochastically (Brownian motion) in a near-harmonic potential well following Ref. 12. Such calculations indicate that the escape probability of the complex is very low, making single-molecule detection potentially possible with the method. Naturally, there are other experimental factors, such as collisions by passing single spheres that might reduce the sensitivity. Accurate quantitative determination of separation efficiency will be the topic of a forthcoming investigation.

For completeness, the possibility of production of false doublets due to scattering acoustic forces (Bjerknes' forces) will be briefly considered. In the velocity antinodes, the Bjerknes' forces may be attractive, making the creation of false doublets a possible problem. However, the Bjerknes' forces are effective only at very small sphere–sphere distances. Calculations based on Ref. 2 show that even with

spheres in direct contact, they are typically less than 2% of F_{acoust} and F_{visc}. Thus, we do not expect false doublets to be formed from these forces, especially since electrostatic repulsion between the surface-charged singlets will counteract the attractive Bjerknes' forces.

Finally, a technical comment on the arrangement of the longitudinal ultrasonic trap. A high-intensity acoustic standing-wave field can be generated in different ways. One method is to use two focusing transducers mounted in reverse directions with common focal planes.[12,24] Alternatively, one focusing transducer is combined with a reflector positioned in the focal plane, as in this work. The latter method has the advantage of ease of alignment, both as regards the generation of a stable, high-intensity standing-wave field and the stable positioning of the capillary in the center of this field. However, due to the sub-100% reflectivity of the molybdenum reflector, the two counter-propagating waves are of unequal intensity, allowing the development of acoustic streaming. Fortunately, this problem is limited since the <100-μm-diam glass capillary prohibits the development of radial streaming components, reducing the streaming to the capillary axial dimension. Furthermore, the interaction volume with the high-intensity field is small, which should also reduce the axial streaming. In our experiments, acoustic streaming was observed to produce a slight increase in the axial flow velocity inside the capillary, at a level that is insignificant for results presented in Sec. III. At present it seems unlikely that future applications, requiring accurate control of the flow velocity, will be hindered by the streaming. Should this become an issue, the axial streaming may be eliminated using the confocal two-transducer arrangement, although it requires accurate matching of the two transducers.

VI. CONCLUSIONS

We have developed a capillary ultrasonic trap for size-selective separation of micrometer-sized particles. In a proof-of-principle experiment, differently sized fluorescent latex spheres were used to verify the theoretically calculated forces acting on the spheres inside the capillary. The experimental results indicate a good separation efficiency of 4.7 from 3.0-μm-diam spheres, but, in order to separate particles of more similar sizes, the uniformity of the velocity distribution inside the capillary must be improved. The long-term goal of the trap is rapid in-flow detection of trace amounts of proteins and other macromolecules, by trapping and detecting latex-sample-latex complexes among single latex spheres. Compared to conventional CE, the capillary ultrasonic trap would not only allow separation, but also in-flow sample-enrichment at spatially specified positions inside the capillary. This will enable long enrichment and detection times, and might improve the limit of detection, potentially to the single-molecule level.

ACKNOWLEDGMENTS

The authors gratefully acknowledge the assistance of Kjell Carlsson and Nils Åslund as regards fluorescence detection, the contributions by Petter Östlund and Henrik Nilsson in the initial phase of this project, Gustav Amberg for sharing his hydrodynamics expertise, and Kjell Hammarström, Rolf Helg, and Frantisek Vykopal for mechanical and electronic support. This project was supported by the Engineering Science Research Council.

[1] E. H. Brandt, Science **243**, 349 (1989).
[2] M. Gröschl, Acustica **84**, 432 (1998).
[3] L. A. Crum, J. Acoust. Soc. Am. **50**, 157 (1971).
[4] Z. Zhu and R. E. Apfel, J. Acoust. Soc. Am. **78**, 1796 (1985).
[5] M. A. H. Weiser and R. E. Apfel, J. Acoust. Soc. Am. **71**, 1261 (1982).
[6] W. T. Coakley, Trends Biotechnol. **8**, 506 (1997).
[7] J. J. Hawkes, M. S. Limaye, and W. T. Coakley, J. Appl. Microbiol. **82**, 39 (1997).
[8] N. E. Thomas, M. A. Sobanski, and W. T. Coakley, Ultrasound Med. Biol. **25**, 443 (1999).
[9] D. A. Johnson and D. L. Feke, Sep. Technol. **5**, 251 (1995).
[10] S. Gupta, D. L. Feke, and I. Manas-Zloczower, Chem. Eng. Sci. **50**, 3275 (1995).
[11] K. Yasuda and S. Umemura, J. Acoust. Soc. Am. **99**, 1965 (1995).
[12] H. M. Hertz, J. Appl. Phys. **78**, 4845 (1995).
[13] M. Petersson, J. Nilsson, L. Wallman, T. Laurell, J. Johansson, and S. Nilsson, J. Chromatogr., B **714**, 39 (1998).
[14] H. J. Issaq, Electrophor. **21**, 1921 (2000).
[15] A. T. Timperman, K. Khatib, and J. V. Sweedler, Anal. Chem. **67**, 139 (1995).
[16] T. Johansson, M. Petersson, J. Johansson, and S. Nilsson, Anal. Chem. **71**, 4190 (1999).
[17] Z. Rosenzweig and E. S. Yeung, Anal. Chem. **66**, 1771 (1994).
[18] T. L. Tolt and D. L. Feke, Analysis and Application of Acoustics to Suspension Processing, in *Proceedings of the 23rd Intersociety Energy Conversion Engineering Conference*, D. Y. Goswami, Ed. (American Society of Mechanical Engineers, New York, 1988), Vol. 4, p. 327.
[19] H. Nilsson, P. Östlund, H. M. Hertz, and S. Nilsson, Detection of Trace Amounts of Protein using Latex-bound Monoclonal Antibodies, in *12th International Symposium on High Performance Capillary Electrophoresis, HPCE'99*, Palm Springs, CA, 23–28 Jan 1999, Abstract L045.
[20] T. Hatano, T. Kaneta, and T. Imasaka, Anal. Chem. **69**, 2711 (1997).
[21] A. R. Selfridge, IEEE Trans. Sonics Ultrason. **32**, 381 (1985).
[22] W. Wang, Y. Liu, G. J. Sonek, M. W. Berns, and R. A. Keller, Appl. Phys. Lett. **67**, 1057 (1995).
[23] G. K. Batchelor, J. Fluid Mech. **74**, 1 (1976).
[24] J. Wu, J. Acoust. Soc. Am. **89**, 2140 (1991).